Available online at www.sciencedirect.com
ScienceDirect
Journal of Solid State Chemistry 180 (2007) 1512–1518
JOURNAL OF SOLID STATE CHEMISTRY
www.elsevier.com/locate/jssc

Nature of the chemical bond and prediction of radiation tolerance in pyrochlore and defect fluorite compounds

Gregory R. Lumpkin[a,b,*], Miguel Pruneda[a], Susana Rios[a], Katherine L. Smith[b], Kostya Trachenko[a], Karl R. Whittle[a,d], Nestor J. Zaluzec[c]

[a]*Cambridge Centre for Ceramic Immobilisation, Department of Earth Sciences, University of Cambridge, Downing Street, Cambridge CB2 3EQ, UK*
[b]*Institute of Materials and Engineering Science, Australian Nuclear Science and Technology Organisation, Private Mail Bag 1, Menai, NSW 2234, Australia*
[c]*Materials Science Division, Argonne National Laboratory, 9700 South Cass Avenue, Argonne, IL 60439, USA*
[d]*Department of Engineering Materials, University of Sheffield, Sir Robert Hadfield Building, Mappin Street, Sheffield S1 3JD, UK*

Received 25 September 2006; received in revised form 24 January 2007; accepted 27 January 2007
Available online 8 February 2007

Abstract

The radiation tolerance of synthetic pyrochlore and defect fluorite compounds has been studied using ion irradiation. We show that the results can be quantified in terms of the critical temperature for amorphization, structural parameters, classical Pauling electronegativity difference, and disorder energies. Our results demonstrate that radiation tolerance is correlated with a change in the structure from pyrochlore to defect fluorite, a smaller unit cell dimension, and lower cation–anion disorder energy. Radiation tolerance is promoted by an increase in the Pauling cation–anion electronegativity difference or, in other words, an increase in the ionicity of the chemical bonds. A further analysis of the data indicates that, of the two possible cation sites in ideal pyrochlore, the smaller *B*-site cation appears to play the major role in bonding. This result is supported by *ab initio* calculations of the structure and bonding, showing a correlation between the Mulliken overlap populations of the *B*-site cation and the critical temperature.

Keywords: Radiation damage; Pyrochlore; *Ab initio*

1. Introduction

Pyrochlore is important in nature as an ore mineral (Nb and Ta) and as a carrier of lanthanide and actinide (Th and U) elements in the Earth's crust. The structure type exhibits a range of useful properties for materials science applications including ionic conductivity (both cations and anions), electrical conductivity, and magnetic properties [1–3]. Pyrochlore is also one of the principal actinide host phases in oxide ceramics designed for the safe disposal of actinide-rich wastes derived from nuclear power generation and the nuclear weapons programs [4–6]. The pyrochlore structure type also has a high tolerance for impurities, is capable of very high waste loadings, and shows excellent chemical durability in aqueous fluids [7–9].

One major concern for these structure types is that they will undergo a crystalline to amorphous transformation as a function of the cumulative alpha decay dose over time. This may lead to volume expansion, cracking, and reduced chemical durability of the waste form. Radiation damage in these materials has been studied using samples doped with short-lived ^{238}Pu (half-life = 87 years) or ^{244}Cm (half-life = 18 years) [10–12], natural samples [13–15], and ion irradiation techniques [16–24]. Although actinide doping experiments are the most relevant to real waste forms, the experiments are difficult, expensive, and limited in scope. Studies of natural pyrochlores also provide complementary information on the long-term behavior in geological environments, but in many cases it is difficult to determine the time–temperature history. In recent years, a number of investigators have chosen to simulate the damage produced by alpha decay processes using ion irradiation techniques, especially the in situ ion irradiation method using thin transmission electron microscope (TEM) specimens.

*Corresponding author.
E-mail address: grl@ansto.gov.au (G.R. Lumpkin).

0022-4596/$ - see front matter © 2007 Elsevier Inc. All rights reserved.
doi:10.1016/j.jssc.2007.01.028

The ion irradiation studies noted above have identified some of the trends of composition and structure with respect to the critical amorphization dose (D_c) and the critical temperature (T_c), above which the material remains crystalline. Results of these studies reveal increasing radiation tolerance (decreasing T_c) as the pyrochlore structure becomes more fluorite-like [25–29]. It should be noted that the structural data and A–B cation radius ratios (R_A/R_B) are not sufficient to explain all of the observed differences in radiation tolerance [30]. In this paper, we illustrate the relationships between T_c and various structural, bonding, and energy parameters. These relationships are presented in the form of empirical equations for the prediction of the critical temperature of pyrochlore and defect fluorite compounds (Fig. 1).

2. Crystal structure of pyrochlore

The pyrochlore structure is a superstructure of the fluorite (MX_2) structure, and is based upon a $2\times2\times2$ supercell containing M_4O_8, with ordered vacancies in the oxide anionic lattice. The space-group symmetry of pyrochlore is $Fd3m$ (no. 227), while that of the parent fluorite structure is $Fm3m$ (no. 225). The structural formula of ideal, stoichiometric pyrochlore can be written as $^{VIII}A_2^{VI}B_2^{IV}X_6^{IV}Y$ in which A and B represent cations, X and Y represent anions, and the Roman numeral superscripts refer to their coordination numbers. In detail, the local coordination environments of each site are AX_6Y_2, BX_6, XA_2B_2, and YA_4 [31,32].

The A cation is located on 16c (0 0 0) and the B cation is located on 16d ($\frac{1}{2}\frac{1}{2}\frac{1}{2}$) in origin choice 2 (at center of symmetry) of space group $Fd3m$. There are three crystallographically distinct anion sites in the pyrochlore lattice, these are the 48f ($x\frac{1}{8}\frac{1}{8}$), 8a ($\frac{1}{8}\frac{1}{8}\frac{1}{8}$), and 8$b$ ($\frac{3}{8}\frac{3}{8}\frac{3}{8}$) sites. In ideal pyrochlore, the oxygen atoms are ordered onto 48f and 8a sites and the 8b site is vacant, allowing the adjacent 48f anions to relax toward the vacant site. This results in the value of the x48f coordinate changing from 0.375 in the ideal fluorite structure to values near 0.33 for a large number of oxide pyrochlores. With increasing R_A/R_B, generally above values of 1.78, certain pyrochlores are found to possess the defect fluorite structure. This is the result of disordering of the A and B cations and disordering of the anions to give occupancies of 0.875 on the 48f, 8a, and 8b sites. In pyrochlore solid-solutions with R_A/R_B approaching 1.78, this disordering process may be continuous (albeit non-linear) and is accompanied by a change in x48f toward 0.375. Thus, many of these pyrochlores are partially disordered [1].

3. Experimental data and statistical analysis

The data discussed in this paper have been obtained by a number of investigators primarily for pyrochlores with A = Y and lanthanides and B = Ti, Sn, Zr, and Hf [17–31]. Experiments were conducted using in situ irradiation of thin TEM samples using 1.0 MeV Kr or in certain cases 1.5 MeV Kr ions at the IVEM-Accelerator Facility, Argonne National Laboratory, USA [33]. Fig. 2 shows the critical temperatures of pyrochlore compounds plotted against the cation–anion radius ratio (R_M/R_X), where M represents the average radius of the A and B cations.

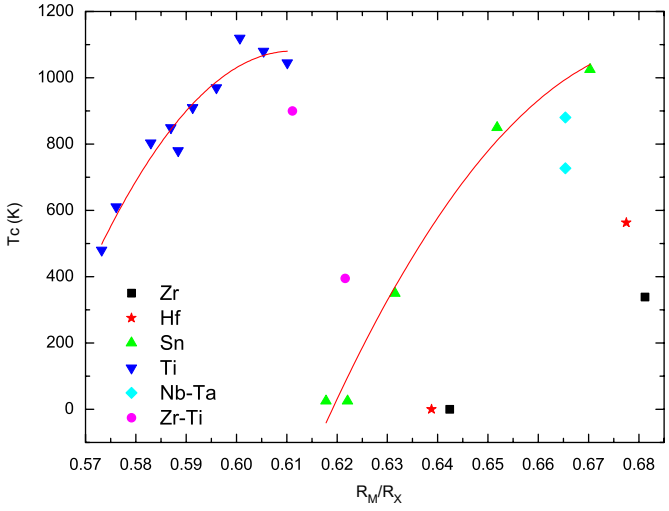

Fig. 2. Plot of the average metal cation (M) to anion radius ratio (R_M/R_X) versus the critical amorphization temperature (T_c) for 21 III–IV pyrochlore compounds plus two natural pyrochlores $NaCaNb_2O_6F$ and $NaCaTa_2O_6F$ (diamonds). The $Ln_2Ti_2O_7$ and $Ln_2Sn_2O_7$ series are delineated by the curves.

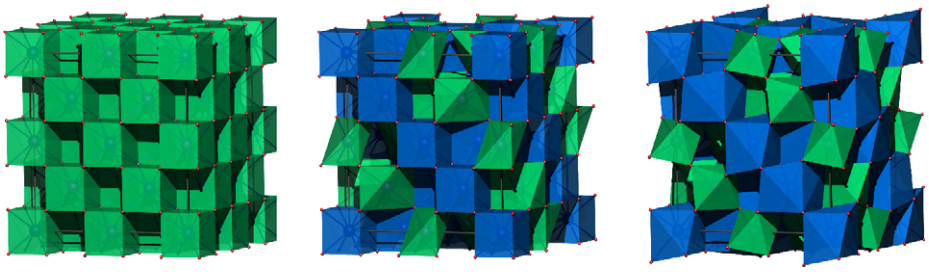

Fig. 1. Crystal structures of fluorite, ordered defect fluorite, and pyrochlore. The fluorite structure shows the cubic nature of the anion coordination around the disordered cations. The defect fluorite shows the effect or removing the 8a anion from the lattice, with x(48f) remaining at 0.375, with the eight coordinated A-site shown in blue and the six coordinated B-site shown in green. The pyrochlore structure shows the effect of the 48f relaxation from 0.375 to 0.3125. The spheres in all structures show the location of the oxygen anions in the lattice.

This is a convenient method of plotting as the data sets are well separated and are related to structural stability according to Pauling's rules (e.g., increased cation coordination and phase transformation is favored by increasing R_M/R_X values). All of the lanthanide titanate pyrochlores shown in Fig. 2 can be amorphized with critical temperatures above about 450 K. The radiation response appears to be non-linear and may roll over at the cubic–monoclinic phase transformation which occurs between $Sm_2Ti_2O_7$ and $Nd_2Ti_2O_7$. Data for lanthanide stannate pyrochlores also appear to exhibit non-linear behavior; however, in this case the compounds with lanthanides heavier than Dy–Ho are resistant to amorphization. The hafnate and zirconate pyrochlores with lanthanides heavier than Gd are radiation resistant.

Multiple linear regression methods were used to conduct a statistical analysis of the critical temperature for 19 different pyrochlore and defect fluorite compounds, in this instance with T_c as the dependent variable. The *X*-anion coordinate ($x48f$), unit cell edge (a_0), *A*–*B* cation radius ratio (R_A/R_B), cation–anion radius ratio (R_M/R_X), average anion–cation Pauling electronegativity difference (ΔX_p), and combined cation–anion disorder energy (E_{dis}) were used as the independent variables. Values for the latter were obtained from the *ab initio* calculations of Grimes and co-workers [32,33]. In this work, we have used the $x48f$ scale ranging from 0.3125 for perfect pyrochlore to 0.375 for defect fluorite. Among these variables both simple negative and positive correlations are observed between T_c and $x48f$ and T_c and R_A/R_B, respectively. These relationships have been recently discussed in the literature [26,30]. More complex correlations are observed for T_c and the other independent variables a_0, R_M/R_X, ΔX_p, and E_{dis}. Note that the useful combinations of independent variables are limited due to high statistical correlations between certain pairs of variables (e.g., $R = 0.99$ for a_0 and R_M/R_X, $R = 0.92$ for R_A/R_B and E_{dis}). The best statistical model derived from these data relates the critical temperature to the following structural, bonding, and energy parameters:

$$T_c = -29738.6(x48f) + 8457.7(a_0) - 1148.9(\Delta X_p) + 939.7(E_{dis}). \quad (1)$$

The model shown above is highly significant with $R^2 = 0.991$ and a standard deviation of 82 K for the predicted value of the critical temperature. Furthermore, all of the independent variables are highly significant as shown by the magnitude of the Student's *t*-test, which lies between 5 and 15 for these four parameters. A plot (not shown) of the calculated versus observed critical temperatures for the pyrochlore and defect fluorite compounds used in the model indicates that there is excellent agreement between the model and observed T_c values across the observed temperature range. This plot also shows that the critical temperatures [21] of the natural pyrochlores $NaCaNb_2O_6F$ and $NaCaTa_2O_6F$ are predicted to within 60 and 150 K, respectively, suggesting that this or a similar model might be applicable to pyrochlore compounds in general.

In order to further investigate the effects of bonding, we performed multiple regression analyses using the individual electronegativities of the *A* and *B* cations, X_{pA} and X_{pB}, instead of the average cation–anion electronegativity difference. Retaining the same set of independent variables used in the development of Eq. (1), the best model that we obtained is as follows:

$$T_c = -33218.6(x48f) + 6722.9(a_0) + 571.8(X_{pB}) + 866.3(E_{dis}). \quad (2)$$

This model includes the same structural and energy terms as in Eq. (1) and also returns a similar level of statistical significance, with $R^2 = 0.991$, a standard deviation of 81 K for the predicted value of the critical temperature, and robust Student's *t* values. Notice that the sign of the electronegativity term in Eq. (2) is now positive. This is because we have used the electronegativity of the cation itself instead of the difference in electronegativities between the cation and anion. Inclusion of X_{pA} in the equation does not significantly improve the regression statistics. This parameter was rejected on the basis of the *t* value of 1.06. Therefore, it appears from this analysis that the electronegativity of the B cation has the most significant correlation with radiation tolerance.

Using the empirical model represented by Eq. (1) and structural data for 51 different compositions, we have determined the T_c response surface for III–IV pyrochlores as a function of the ionic radii of the *A* cation (Y and lanthanides) and *B* cation (Ti, Mo, Sn, Hf, Zr). Fig. 3 is a two-dimensional contour map of the predicted critical temperature, illustrating that the response surface is a

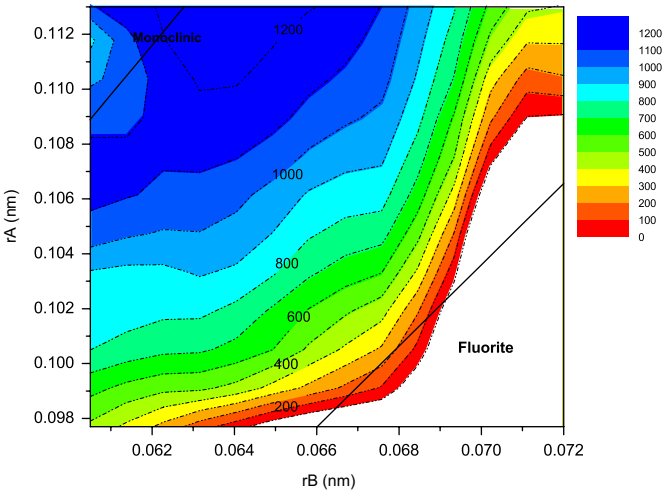

Fig. 3. Contour map of the predicted critical amorphization temperature for III–IV pyrochlore compounds versus the *A*-site and *B*-site cation radii. Contours of T_c are shown in degrees Kelvin. This figure was constructed using data for pyrochlores with *A* = La–Lu plus Y and *B* = Ti, Mo, Sn, Hf, and Zr. The range of pyrochlore stability are shown and labeled as monoclinic and fluorite.

complex function of the material properties in this region of the III–IV pyrochlore composition space. Notice that the T_c contours curve upwards toward the right side of the figure in the vicinity of the larger B cations. This curvature reflects the increasing radiation resistance of pyrochlore and defect fluorite compounds with increasing B cation size (e.g., Sn, Hf, and Zr).

The three-dimensional form of the radiation response surface is shown in Fig. 4. Here, we see that the surface rises steeply from 0 K and then levels off at high temperatures for the compositions with large A-site and small B-site cation radii. The form of the surface shown in Fig. 4 also reflects, to a certain extent, the non-linear trends of the Ti and Sn data sets plotted in Fig. 2. Based upon this curvature, we suggest that the T_c values of the $Ln_2Ti_2O_7$ compounds may begin to decrease beyond the cubic–monoclinic phase transition within the stability field of the monoclinic layered perovskites with Ln = Nd, Pr, Ce, and La.

4. *Ab initio* calculations

We carried out first principles calculations of the structures of selected pyrochlore and defect fluorite compounds with A = Y, La and B = Ti, Zr, Sn, Hf. These calculations were performed using SIESTA, a self-consistent implementation of density functional theory in combination with the pseudo-potential approximation to remove core electrons from consideration [34]. From these data, we have calculated the Mulliken overlap populations as a measure of the A–O and B–O bonds (Table 1).

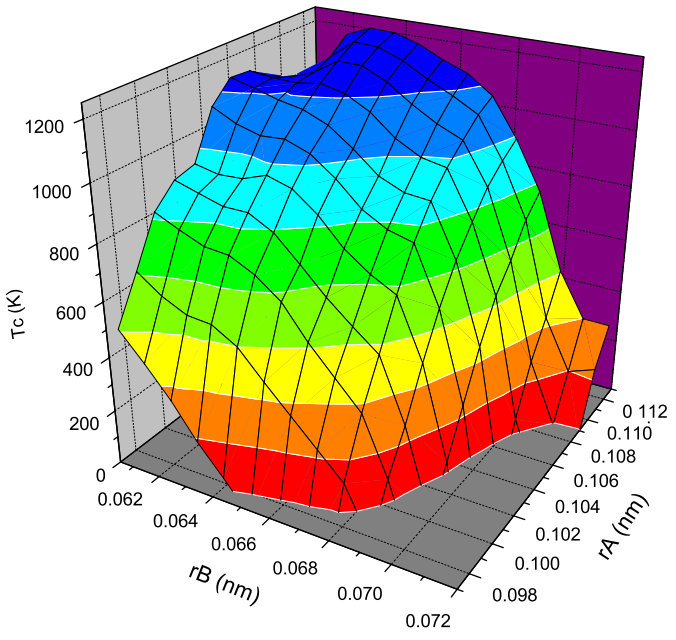

Fig. 4. Three-dimensional representation of the predicted critical amorphization temperature. This figure shows the approximate form of the surface and suggests that the critical temperature levels off, possibly decreasing in the field of the monoclinic structure types with A = Nd–La.

Mulliken overlap populations are frequently used as a measure of ionicity/covalency, where greater overlap (larger numerical value in Table 1) indicates increased covalency.

In general, the results are reasonable given the uncertainties involved in the calculations for these relatively complex oxides. Although the calculated value of the Mulliken overlap population for Hf seems high relative to Zr, the result does provide an explanation for the large difference in T_c between $La_2Zr_2O_7$ (339 K) and $La_2Hf_2O_7$ (563 K) given that the structures of these two pyrochlores are nearly identical [35].

For the La compounds listed in Table 1, the data show that the ionicity of the B–O bonds increases in the order Sn < Hf < Zr (note that $La_2Ti_2O_7$ is not a pyrochlore, it is a layered perovskite structure type similar to $Ca_2Nb_2O_7$). In comparison, the Pauling electronegativity data indicate that the ionicity should increase in the order Sn < Zr < Hf, although the individual electronegativities of Zr (1.33) and Hf (1.30) are quite close to one another. This is not an unusual result, as the electronegativity scales are very general and cannot be expected to predict the detailed behavior of different compounds in every case. Nevertheless, the results presented here suggest that bonding effects are dominant for the La compounds, as there are only minor differences in the X-anion coordinate and disorder energies (see Table 1).

Table 1 also shows that Y and La have a similar level of ionicity (M_{A-O} = 0.026–0.041) in all eight compounds, with the Y–O bonds being consistently slightly more ionic than the La–O bonds. This is an important result, since the structure of pyrochlore can also be viewed as two interpenetrating networks, a B_2X_6 octahedral framework with hexagonal tungsten bronze-type layers on (1 1 1) planes and an anti-cristobalite type A_2Y network [32]. Thus, it appears that the nature of the bonding of the B_2X_6 framework exerts a major control on radiation tolerance in these compounds. This result is in agreement with the empirical model of Eq. (2). Upon examination of the data for the Y compounds, we note that $Y_2Ti_2O_7$ does not fit the picture derived from the Mulliken overlap populations alone. Further examination of Table 1 shows the structural and disorder energy parameters which show much larger differences for these four compounds. In particular, $Y_2Ti_2O_7$ has the lowest X-anion coordinate (more pyrochlore-like) and the highest disorder energy, suggesting that these parameters are dominant over bonding effects. This is consistent with the form of the T_c surface shown in Figs. 3 and 4.

5. Discussion and conclusions

This study shows that radiation damage data can be statistically quantified as a function of structural, bonding, and disorder energy parameters. Furthermore, based upon the available data for two natural pyrochlore samples, we show that the statistical approach may be generally

Table 1
Mulliken overlap populations (M) for A–O and B–O bonds of pyrochlore compounds with A = Y, La and B = Ti, Zr, Sn, and Hf

Compound	M_{A-O}	M_{B-O}	ΔX_p (A)	ΔX_p (B)	$x48f$	E_{dis} (eV)	T_c (K) observed
$Y_2Sn_2O_7$	0.026	0.202	1.22	1.96	0.337	3.6	—
$Y_2Ti_2O_7$	0.027	0.111	1.22	1.54	0.330	4.8	780
$Y_2Hf_2O_7$	0.029	0.090	1.22	1.30	*0.375*	3.0	—
$Y_2Zr_2O_7$	0.026	0.017	1.22	1.33	*0.375*	2.8	—
$La_2Sn_2O_7$	0.034	0.207	1.10	1.96	0.329	4.2	1025
$La_2Ti_2O_7$	0.036	0.110	1.10	1.54	—	—	—
$La_2Hf_2O_7$	0.041	0.096	1.10	1.30	0.331	4.1	563
$La_2Zr_2O_7$	0.037	0.027	1.10	1.33	0.332	4.0	339

Larger values of the overlap population are related to increased covalency, e.g., sharing of electrons via overlapping atomic orbitals between atoms.

applicable to stoichiometric pyrochlores with a range of A-site and B-site cation valence combinations. The statistical analysis given above indicates that structural aspects are important contributors to radiation tolerance. In the case of the pyrochlore structure, the topological element ($x48f$ parameter) describes the change from pyrochlore-like to fluorite-like geometry. It is well known that this topological change is associated with increased oxygen ion conductivity [1], a factor that may contribute to enhanced defect mobility and recombination in thin films during ion irradiation. This is particularly true of the materials studied in this paper, whereby ionic conductivity may be enhanced by several orders of magnitude upon the development of anion disorder over the 48f, 8a, and (normally vacant) 8b sites.

Radiation tolerance and structural aspects are also related to the concept of structural freedom, f, and its relationship to topological disorder as discussed by Hobbs et al. [36]. In this concept the characteristic structural units are the coordination polyhedra each having V vertices and the connectivity, C, is defined as the average number of polyhedra sharing each vertex. The latter can be further described by the relative proportions of edges and faces shared with other polyhedra. Effectively, the structural freedom is the difference between the degrees of freedom given by the structure dimensionality and the number of constraints imposed by the connectivity. This is represented by the equation below, in which d is the dimensionality of the structure, δ is the dimensionality of the polyhedron (or "polytope"), Y is the fraction of edge-sharing vertices, and Z is the fraction of vertices sharing faces with p sides:

$$f = d - C\left\{\delta - \left[\frac{\delta(\delta+1)}{2V}\right]\right\} - (d-1)\left(\frac{Y}{2}\right) - [(p-1)d - (2p-3)]\left(\frac{Z}{p}\right).$$

In the case of pyrochlore-defect fluorite compounds (and many other structures types), the topological degrees of freedom may be calculated from the entire structure or from the major structural elements, e.g., the B_2X_6 framework or A_2Y network. In ideal fluorite, the structural freedom derived from the whole structure is −7.0. In the case of pyrochlore, the value of $f = -6.1$ for the whole structure, whereas the B_2X_6 and A_2Y networks give values of −1.0 and 0.0, respectively. If one or the other of these networks exerts a dominant effect on the properties of the crystal, then the "apparent" f value might be considerably greater than that calculated for the whole structure. It has been suggested previously that the B_2X_6 framework is the main structural element and this is in accord with the range of known defect pyrochlores. Furthermore, the *ab initio* calculations suggest that the A_2Y network is generally ionic in nature (low Mulliken overlap population) whereas the bonding of the B_2X_6 framework changes according to the nature of the B-site cation. These results indicate, everything else being equal, that the radiation tolerance follows the order fluorite > defect fluorite > pyrochlore. This is in general agreement with the data for the X-anion coordinate and disorder energies.

The empirical models described in this paper also demonstrate that electronegativity (and therefore ionicity) is an important parameter, particularly in the case of the B-site cation. This result confirms the bond-type criterion proposed by Naguib and Kelly [37], who showed a broad correlation between electronegativity and radiation tolerance. A recent review of radiation damage effects in oxide pyrochlores by Ewing and co-workers [38] has further illustrated the importance of electronic structure and bonding through comparison of different compositions (e.g., $Gd_2Sn_2O_7$ and $Gd_2Hf_2O_7$) with otherwise similar properties such as the A–B cation radius ratio. Trachenko [39] has given a more general review of the physics of radiation damage where it is suggested that short-range covalent and long-range ionic contributions to the total force field between any given pair of atoms interact to produce a "landscape" of potential energy. The full three-dimensional expression of this landscape, with its various energy minima (and activation barriers) in a crystal determines the ability to recover the disorder produced by an atomic collision cascade. In general, short-range covalent contributions lead to highly directional bonds (e.g., orbital hybridization, polyhedral distortion) and a number of distinct potential energy minima which act as barriers to recovery of periodicity in the vicinity of the collision cascade. Long-range ionic contributions tend to

simplify the energy landscape, thereby minimizing the barriers to recovery of atomic periodicity. The empirical models and *ab initio* calculations discussed in the present work both support the role of ionicity in promoting radiation tolerance in pyrochlore compounds.

The positive correlation between T_c and the combined cation–anion disorder energy is consistent with the contour plots reported in the literature [32,33]. These calculations indicate that E_{dis} decreases with decreasing A-site cation radius and increasing *B*-site cation radius, where radiation tolerant defect fluorite structures are encountered in the III–IV pyrochlore composition space. Comparison of Figs. 3 and 5 in Minervini et al. [32] show that the degree of correlation between the critical temperature and the disorder energy increases for the larger *B*-site cations. When examined in detail, we see that the contour lines of the disorder energy are nearly vertical for the smaller *B*-site cations. Thus, the disorder energy appears to play a more important role in promoting radiation resistance with increasing *B*-site cation radius in this system.

In conclusion, the radiation tolerance of pyrochlore and defect fluorite compounds can be described by a combination of structural, bonding, and energetic parameters. The results of this study apply strictly to thin crystals of these materials irradiated with 1.0–1.5 MeV Kr ions, as the radiation response is known to vary as a function of ion mass, energy, and in some cases ion flux (e.g., the rate of ions hitting the sample) [38,40]. For the compounds considered in this work, the effects of ion mass and energy remain to be examined in detail. The challenge ahead is to understand these relationships in greater detail, both within the field of a given structure type and across the phase boundaries into the fields of neighboring compounds. In order to accomplish the latter part of this task, a set of universal structural parameters (e.g., volume and structural distortion) must be found.

Acknowledgments

We are grateful to R.C. Ewing and his staff of the University of Michigan and W.J. Weber at the Pacific Northwest National Laboratory (PNNL) for previous collaborations and discussions of radiation damage in pyrochlore and related compounds. This work would not have been possible without the assistance of R.C. Birtcher, C.W. Allen, and staff members of the IVEM-Accelerator Facility, Argonne National Laboratory.

References

[1] C. Heremans, B.J. Wuensch, J.K. Stalick, E. Prince, J. Solid State Chem. 117 (1995) 108.
[2] O. Vyaselev, K. Arai, J. Yamazaki, M. Tagikawa, M. Hanawa, Z. Hiroi, Phys. B: Condens. Matter 329 (2003) 959.
[3] N.P. Raju, M. Dion, M.J.P. Gingras, T.E. Mason, J.E. Greedan, Phys. Rev. B 59 (1999) 14489.
[4] C.J. Ball, W.J. Buykx, F.J. Dickson, K.D. Hawkins, D.M. Levins, R.S.C. Smart, K.L. Smith, G.T. Stevens, K.G. Watson, D. Weedon, T.J. White, J. Am. Ceram. Soc. 72 (1989) 404.
[5] F.J. Dickson, H. Mitamura, T.J. White, J. Am. Ceram. Soc. 72 (1989) 1055.
[6] R.C. Ewing, W.J. Weber, F.W.J. Clinard, Prog. Nucl. Energy 29 (1995) 63.
[7] G.R. Lumpkin, J. Nucl. Mater. 289 (2001) 136.
[8] G.R. Lumpkin, K.L. Smith, R. Gieré, C.T. Williams, Geochemical behaviour of host phases for actinides and fission products in crystalline ceramic nuclear waste forms, in: R. Gieré, P. Stille (Eds.), Energy, Waste and the Environment: A Geochemical Perspective, vol. 236, Geological Society, London, 2004, p. 89.
[9] J.P. Icenhower, D.M. Strachan, M.M. Lindberg, E.A. Rodriguez, J.L. Steele, Dissolution Kinetics of Titanate-Based Ceramic Waste Forms: Results from Single-Pass Flow Tests on Radiation Damaged Specimens, Pacific Northwest National Laboratory, 2003.
[10] J.W. Wald, P. Offerman, A study of radiation effects in curium-doped $Gd_2TI_2O_7$ (pyrochlore) and $CaZrTi_2O_7$ (zirconolite). Scientific Basis for Nuclear Waste Management V, 1982, Berlin.
[11] F.W.J. Clinard, D.E. Peterson, D.L. Rohr, L.W. Hobbs, J. Nucl. Mater. 126 (1984) 245.
[12] W.J. Weber, J.W. Wald, H. Matzke, J. Nucl. Mater. 138 (1986) 196.
[13] G.K. Krivokoneva, G.A. Sidorenko, Geochem. Int. 8 (1971) 113.
[14] G.R. Lumpkin, R.C. Ewing, Phys. Chem. Min. 16 (1988) 2.
[15] G.R. Lumpkin, K.P. Hart, P.J. McGlinn, T.E. Payne, R. Gieré, C.T. Williams, Radiochim. Acta 66/67 (1994) 469.
[16] W.J. Weber, N.J. Hess, G.D. Maupin, Nucl. Instrum. Methods Phys. Res. Sect. B—Beam Interact. Mater. Atoms 65 (1992) 102.
[17] K.L. Smith, N.J. Zaluzec, G.R. Lumpkin, J. Nucl. Mater. 250 (1997) 36.
[18] S.X. Wang, L.M. Wang, R.C. Ewing, K.V. Govindana Kutty, Ion irradiation effects for two pyrochlore compositions: $Gd_2Ti_2O_7$ and $Gd_2Zr_2O_7$. Microstructural Processes in Irradiated Materials, 1999.
[19] S.X. Wang, L.M. Wang, R.C. Ewing, G.S. Was, G.R. Lumpkin, Nucl. Instrum. Methods Phys. Res. Sect. B: Beam Interact. Mater. Atoms 148 (1999) 704.
[20] S.X. Wang, B.D. Begg, L.M. Wang, R.C. Ewing, W.J. Weber, K.V.G. Kutty, J. Mater. Res. 14 (1999) 4470.
[21] S.X. Wang, L.M. Wang, R.C. Ewing, J. Non-Cryst. Solids 274 (2000) 238.
[22] G.R. Lumpkin, K.L. Smith, M.G. Blackford, J. Nucl. Mater. 289 (2001) 177.
[23] B.D. Begg, N.J. Hess, D.E. McCready, S. Thevuthasan, W.J. Weber, J. Nucl. Mater. 289 (2001) 188.
[24] A. Meldrum, C.W. White, V. Keppens, L.A. Boatner, R.C. Ewing, Phys. Rev. B 6310 (2001) 104109.
[25] R.C. Ewing, J. Lian, L.M. Wang, Ion Beam-Induced Amorphization of the Pyrochlore Structure Type: A Review. Radiation Effect and Ion Beam Modification of Materials, Boston, 2004.
[26] J. Lian, J. Chen, L.M. Wang, R.C. Ewing, J.M. Farmer, L.A. Boatner, K.B. Helean, Phys. Rev. B 68 (2003) 134107.
[27] J. Lian, R.C. Ewing, L.M. Wang, K.B. Helean, J. Mater. Res. 19 (2004) 1575.
[28] J. Lian, L.M. Wang, R.G. Haire, K.B. Helean, R.C. Ewing, Nucl. Instrum. Methods Phys. Res. Sect B—Beam Interact. Mater. Atoms 218 (2004) 236.
[29] J. Lian, X.T. Zu, K.V.G. Kutty, J. Chen, L.M. Wang, R.C. Ewing, Phys. Rev. B 66 (2002) 054108.
[30] G.R. Lumpkin, K.R. Whittle, S. Rios, K.L. Smith, N.J. Zaluzec, J. Phys.—Condens. Matter 16 (2004) 8557.
[31] C.W. Allen, L.L. Funk, E.A. Ryan, New instrumentation in Argonne's HVEM-tandem, facility: expanded capability for in situ beam studies. Ion-Solid Interactions for Materials Modification and Processing, 1996.

[32] L. Minervini, R.W. Grimes, K.E. Sickafus, J. Am. Ceram. Soc. 83 (2000) 1873.
[33] K.E. Sickafus, L. Minervini, R.W. Grimes, J.A. Valdez, M. Ishimaru, F. Li, K.J. McClellan, T. Hartmann, Science 289 (2000) 748.
[34] K. Trachenko, M. Pruneda, E. Artacho, M.T. Dove, Phys. Rev. B 71 (2005) 184104.
[35] G.R. Lumpkin, K.R. Whittle, S. Rios, K.L. Smith, N.J. Zaluzec, J. Phys.—Condens. Matter 16 (2004) 8557.
[36] L.W. Hobbs, A.N. Sreeram, C.E. Jesurum, B.A. Berger, Nucl. Instrum. Methods Phys. Res. Sect B—Beam Interact. Mater. Atoms 116 (1996) 18.
[37] H.M. Naguib, R. Kelly, Radiat. Eff. 25 (1975) 1.
[38] R.C. Ewing, W.J. Weber, J. Lian, J. Appl. Phys. 95 (2004) 5949.
[39] K. Trachenko, J. Phys. Condens. Matter 16 (2004) R1491.
[40] W.J. Weber, Nucl. Instrum. Methods Phys. Res. Sect. B—Beam Interact. Mater. Atoms 166–167 (2000) 98.